Two Phases of $[Me_4N][Ni(dmise)_2]_2$: Syntheses, Crystal Structures, Electrical Conductivities, and Intermolecular Orbital Overlap Calculations of α- and β-Tetramethylammonium Bis[bis(2-selenoxo-1,3-dithiole-4,5-dithiolato)nickelate], the First Conductors Based on the $M(C_3S_4Se)_2$ System

Joost P. Cornelissen,[1a] Brigitte Pomarède,[1b] Anthony L. Spek,[1c] Derk Reefman,[1d] Jaap G. Haasnoot,*[,1a] and Jan Reedijk[1a]

Department of Chemistry, Gorlaeus Laboratories, Leiden University, P.O. Box 9502, 2300 RA Leiden, The Netherlands, Laboratoire de Chimie de Coordination du CNRS, Unité No. 8241 liée par conventions à l'Université Paul Sabatier et à l'Institut National Polytechnique de Toulouse, 205 Route de Narbonne, 31077 Toulouse Cedex, France, Vakgroep Kristal- en Structuurchemie, Bijvoet Center for Biomolecular Research, Utrecht University, Padualaan 8, 3584 CH Utrecht, The Netherlands, and Department of Physics, Kamerlingh Onnes Laboratories, Leiden University, P.O. Box 9506, 2300 RA Leiden, The Netherlands

Received December 29, 1992

Electrochemical oxidation of a solution of $[Me_4N][Ni(dmise)_2]$ (dmise = $C_3S_4Se^{2-}$ = 2-selenoxo-1,3-dithiole-4,5-dithiolate) yields platelet-shaped crystals of α-$[Me_4N][Ni(dmise)_2]_2$ (**I**). Electrooxidation of $[Bu_4N][Ni(dmise)_2]_2$ in the presence of a large excess of Me_4NPF_6 yields both α-$[Me_4N][Ni(dmise)_2]_2$ and needle-shaped crystals of β-$[Me_4][Ni(dmise)_2]_2$ (**II**). Single-crystal X-ray measurements were carried out for both compounds. Compound **I** crystallizes in the orthorhombic space group *Pbnb*, with a = 7.3617(7) Å, b = 11.6824(9) Å, c = 39.004(2) Å, V = 3354.4(4) Å^3, and Z = 4 for $C_{16}H_{12}NNi_2S_{16}Se_4$. Compound **II** crystallizes in the monoclinic space group $C2/c$, with a = 14.1465(7) Å, b = 6.4999(4) Å, c = 36.553(2) Å, β = 95.580(4)°, V = 3345.1(3) Å^3, and Z = 4 for $C_{16}H_{12}NNi_2S_{16}Se_4$. Direct methods were used for the structure determinations, and both structures were refined by least-squares methods to a residual R_w of 0.072 for 1909 reflections (**I**) and an R_w of 0.051 for 1762 reflections (**II**). In compound **I**, every two $Ni(dmise)_2$ units form diads which are arranged in a nonstacking mode. Each diad is surrounded by six other pairs, forming an acceptor sheet in the *ab* plane. In this plane, many short intermolecular S···S contacts exist. The cations are lying in between the sheets. The $Ni(dmise)_2$ molecules are connected along the *c*-axis via an extremely short terminal Se···Se contact of 3.277(3) Å. In compound **II**, the $Ni(dmise)_2$ units are slightly dimerized and stack along [110] and [1$\bar{1}$0]. They form acceptor layers in the *ab* plane which are separated by the cations. Short intermolecular contacts can be found within these layers. Conductivity measurements indicate room temperature values of 1 S cm^{-1} (**I**) and 10 S cm^{-1} (**II**). Both compounds behave as semiconductors with E_a = 0.08 eV (**I**) and 0.05 eV (**II**), as evident from temperature-dependent conductivity measurements. Cyclic voltammetry experiments show that the redox properties of $Ni(dmise)_2$ are comparable to those of the all-sulfur analog. The electrochemical behavior of $Pd(dmise)_2$ differs from that of $Pd(dmit)_2$ in the sense that the oxidation from $[Pd(dmise)_2]^{2-}$ to the mixed-valence state seems to occur in one step. Intermolecular overlap integral calculations were performed for both salts. They indicate a 1-D character for the band structure in salt **I**, in spite of its nonstacking molecular arrangement. In structure **II**, the larger interplanar spacing of the $Ni(dmise)_2$ molecules results in smaller molecular orbital overlap values than in the all-sulfur analog $[Me_4N][Ni(dmit)_2]_2$.

Introduction

One of the basic requirements for obtaining high conductivity in molecular materials is the formation of an effective electronic conduction band. This can be achieved by introducing a large number of chalcogen atoms on the periphery of the molecules. The success of the formally inorganic molecular conductors based on the square-planar $M(dmit)_2$ system (with M = Ni, Pd, and Pt and dmit = $C_3S_5^{2-}$ = 2-thioxo-1,3-dithiole-4,5-dithiolate), some of which are known as high-pressure superconductors,[2,3] lies therefore in the fact that in these salts a large number of intermolecular interactions through the sulfur atoms of the dmit ligands can occur. One of the methods to further increase the intermolecular orbital overlap and, possibly, also the dimensionality of the conduction pathway is in substitution of sulfur by selenium. The selenium atom possesses spatially more extended orbitals and has a greater polarizability compared to sulfur.

In the past, several selenium-containing analogs of dmit have been prepared.[3-9] The all-selenium ligand dsis (= $C_3Se_5^{2-}$ =

* To whom correspondence should be addressed.

(1) (a) Department of Chemistry, Leiden University. (b) Laboratoire de Chimie de Coordination du CNRS. (c) Utrecht University. (d) Department of Physics, Leiden University.

(2) Cassoux, P.; Valade, L.; Kobayashi, H.; Kobayashi, A.; Clark, R. A.; Underhill, A. E. *Coord. Chem. Rev.* **1991**, *110*, 115 and references therein.

(3) (a) Kobayashi, A.; Kim, H.; Sasaki, Y.; Murata, K.; Kato, R.; Kobayashi, H. *J. Chem. Soc., Faraday Trans. 2* **1990**, *86*, 361. (b) Kobayashi, A.; Kobayashi, H.; Miyamoto, A.; Kato, R.; Clark, R. A.; Underhill, A. E. *Chem. Lett.* **1991**, 2163.

(4) (a) Olk, R.-M.; Dietzsch, W.; Mattusch, J.; Stach, J.; Nieke, N.; Hoyer, E. *Z. Anorg. Allg. Chem.* **1987**, *544*, 199. (b) Matsubayashi, G.; Akiba, K.; Tanaka, T. *J. Chem. Soc., Dalton Trans.* **1990**, 115. (c) Matsubayashi, G.; Yokozawa, A. *J. Chem. Soc., Dalton Trans.* **1990**, 3013. (d) Matsubayashi, G.; Yokozawa, A. *J. Chem. Soc., Dalton Trans.* **1990**, 3535.

(5) (a) Olk, R.-M.; Olk, B.; Rohloff, J.; Hoyer, E. *Z. Chem.* **1990**, *30*, 445. (b) Kobayashi, H.; Kato, R.; Kobayashi, A. *Synth. Met.* **1991**, *42*, 2495. (c) Khodorkovskii, V. Y.; Kreicberga, J.; Balodis, K. A.; Neiland, O. Y. *Isv. Akad. Nauk, Latv. SSR, Ser. Khim.* **1988**, 120. (d) Cornelissen, J. P.; Reefman, D.; Haasnoot, J. G.; Spek, A. L.; Reedijk, J. *Recl. Trav. Chim. Pays-Bas* **1991**, *110*, 345.

(6) Nigrey, P. J.; Morosin, B.; Kwak, J. F. *Novel Superconductivity*; Wolf, S. A., Kresin, V. Z., Eds.; Plenum Press: New York, 1987; p 171.

(7) Nigrey, P. J. *Synth. Met.* **1988**, *27*, B365.

(8) Beno, M. A.; Kini, A. M.; Geiser, U.; Wang, H. H.; Carlson, K. D.; Williams, J. M. *The Physics and Chemistry of Organic Superconductors*; Saito, G., Kagoshima, S., Eds.; Springer Verlag: Berlin, 1990; p 369.

0020-1669/93/1332-3720$04.00/0

Chart I

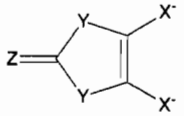

X=Y=Z=S	dmit
X=Y=S, Z=Se	dmise
X=Se, Y=Z=S	dsit
X=Z=Se, Y=S	dsise
X=Y=Z=Se	dsis

2-selenoxo-1,3-diselenole-4,5-diselenolate) and the diselenolato ligand dsit (= $C_3S_3Se_2^{2-}$ = 2-thioxo-1,3-dithiole-4,5-diselenolate) are the ones most studied (Chart I). It was found that the structural and/or electronic properties of square-planar nickel complexes with these ligands can be quite different from those of the corresponding dmit salts. In particular, the substitution of the dithiolate function by diselenolato groups can have a pronounced effect on the redox behavior and the structures of the nickel complexes, e.g. resulting in strong dimerization.[8-10]

One of the selenium-containing dmit analogs which is expected to have properties differing the least from those of dmit is the selenone ligand dmise (= $C_3S_4Se^{2-}$ = 2-selenoxo-1,3-dithiole-4,5-dithiolate, Chart I), since it contains only one bonded selenium atom. Another reason to use this particular ligand is that in some $M(dmit)_2$ salts significant intermolecular S···S interactions via the terminal thioxo groups have been found.[11] Such thioxo contacts could provide an extra dimension of the conduction pathway, namely along the direction of the long molecular axis. A selenoxo group is expected to increase these terminal contacts. Moreover, the greater size of the selenium atoms should lead to an increase in the unit cell volume in salts that remain isostructural upon selenium substitution. This effect would diminish the on-site Coulomb repulsion energy (U) of the system.[12]

Only few studies on the dmise ligand have been reported to date, most of them dealing with its synthetic organic aspects, or with the spectroscopical properties of $[M(dmise)_2]^{2-}$ and $[M(dmise)_2]^-$ salts.[5,9] In this paper we report the synthesis, the structural and electronic properties of the first dmise-based mixed-valence salts, i.e. α- and β-$[Me_4N][Ni(dmise)_2]_2$ (abbreviated **I** and **II**, respectively). These two compounds are the selenone analogs of the superconducting $[Me_4N][Ni(dmit)_2]_2$.[13] Their structures and properties will be compared to each other and to related dmit compounds. In addition, the electrochemical behavior of the $M(dmise)_2$ systems (with M = Ni, Pd) will be described. A preliminary report of the structure and conductivity of α-$[Me_4N][Ni(dmise)_2]_2$ was presented earlier.[5d]

Experimental Section

Synthesis of 4,5-Bis(benzoylthio)-1,3-dithiole-2-selenone (dmise(COPh)$_2$). For the synthesis of 4,5-bis(benzoylthio)-1,3-dithiole-2-selenone two different routes can be followed. The first one involves the synthesis of 1,3-dithiole-2-selenone from 1,3-dithiole-2-thione as the first step, followed by lithiation of the double bond and insertion of sulfur.[7,14,15] The ligand can be stabilized as its zinc chelate and subsequently converted to the target compound by treatment with benzoyl chloride. However, a much faster method for the synthesis of dmise(COPh)$_2$ was published in 1988[5c] and starts from the readily available dmit(COPh)$_2$.[16] The procedure followed by us, and as given in Scheme I, is based on that report.

Scheme I

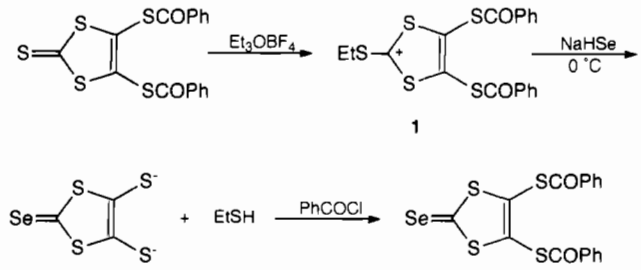

All reaction steps were carried out under argon. First, 10 mL of a 1 M solution of Et_3OBF_4 in CH_2Cl_2 (Aldrich Chemicals) is dropwise added to 4.06 g (10 mmol) of dmit(COPh)$_2$ dissolved in approximately 60 mL of CH_2Cl_2. After the addition is completed, the yellow-red solution is stirred for 1 h at room temperature. Afterward, the solution is cooled in an ice bath and 200 mL of dry diethyl ether is added. The tetrafluoroborate salt **1** (Scheme I) precipitates as light yellow needles upon standing at –20 °C for several hours. The product is collected by filtration, washed with cold diethyl ether, and dried. Elemental analyses were found to be in agreement with the formula $C_{19}H_{15}O_2S_5BF_4$. Yield: 5.17 g (99%).

A solution of NaHSe in 2-propanol can be obtained by adding 1.14 g (30 mmol) of $NaBH_4$ to a vigorously stirred suspension of 1.88 g (24 mmol) of elemental selenium in 200 mL of 2-propanol.[17] B_2H_6 gas evolves, and stirring is continued for 1 h or until all of the selenium has reacted. The clear solution is put in an ice bath and 4.18 g (80 mmol) of salt **1** is added over a period of approximately 30 min. The stirred solution turns dark red-purple, indicative of the liberation of the anionic dithiolate ligand. Ethanethiol forms as a byproduct. When the addition is completed, the mixture is allowed to react for an extra 1.5 h. After this period, a solution of 4 mL (4.7 g) of benzoyl chloride in 10 mL of 2-propanol is dropwise added. A brown powder precipitates. The product is collected by filtration and recrystallized from CH_2Cl_2/methanol. Orange needles are obtained. The elemental analyses were found to be in agreement with formula $C_{17}H_{10}O_2S_4Se$. Mp: 139 °C (Lit. mp 142 °C).[5c] Yield: 1.44 g (40%).

Synthesis of $[Bu_4N]_n[M(dmise)_2]$ (n = 1 or 2; M = Ni or Pd). The metal complexes were prepared in analogy to the syntheses of the corresponding dmit compounds, as described by Steimecke et al.[16]

Synthesis of $[Me_4N][Ni(dmise)_2]$. The $[Me_4N][Ni(dmise)_2]$ salt was prepared from $[Bu_4N][Ni(dmise)_2]$ by cation metathesis. A solution of 1.1 g (10 mmol) of Me_4NCl in approximately 20 mL of dry methanol is added to a stirred solution of 0.79 g (1 mmol) of $[Bu_4N][Ni(dmise)_2]$ in 200 mL of acetone. The mixture is concentrated to a total volume of about 75 mL and cooled in an ice bath. After approximately 50 mL of 2-propanol is added, the solution is left to stand at –20 °C overnight. Shiny, black needles are collected by filtration, washed with cold methanol, and dried. The compound analyzed by $C_{10}H_{12}NNiS_8Se_2$. Yield: 0.52 g (84%).

Electrocrystallization Synthesis of α-$[Me_4N][Ni(dmise)_2]_2$ (I). A solution of 0.06 g (0.097 mmol) of $[Me_4N][Ni(dmise)_2]$ in 30 mL of dry acetonitrile was poured into an H-tube equipped with a fine porosity frit. No extra electrolyte was used. Two platinum electrodes (1 mm diameter) were put in the dark brown solution and a constant current of approximately 2 μA was applied. Black, hexagonal platelets could be isolated from the anode after 4 days. In addition, lustrous, black squares were found on the bottom of the anodic compartment. Both forms proved to be of the same orthorhombic phase.

Electrocrystallization Synthesis of β-$[Me_4N][Ni(dmise)_2]_2$ (II). A solution of 0.039 g (0.05 mmol) of $[Bu_4N][Ni(dmise)_2]$ and 0.11 g (0.5 mmol) of powdered Me_4NPF_6 (Aldrich Chemicals) in 30 mL of dry acetonitrile was poured into an H-tube equipped with a fine-porosity frit. The same electrooxidation conditions as described above were applied. After about 7 days, black, needle-shaped crystals which proved to be of the monoclinic β-phase had grown on the anode, together with black

(9) Olk, R.-M.; Olk, B.; Rohloff, J.; Reinhold, J.; Sieler, J.; Trübenbach, K.; Kirmse, R.; Hoyer, E. *Z. Anorg. Allg. Chem.* **1992**, *609*, 103.
(10) Cornelissen, J. P.; Haasnoot, J. G.; Reedijk, J.; Faulmann, C.; Legros, J.-P.; Cassoux, P.; Nigrey, P. J. *Inorg. Chim. Acta* **1992**, *202*, 131.
(11) Kato, R.; Kobayashi, H.; Kim, H.; Kobayashi, A.; Sasaki, Y.; Mori, T.; Inokuchi, H. *Chem. Lett.* **1988**, 865.
(12) Wang, H. H.; Montgomery, L. K.; Geiser, U.; Porter, L. C.; Carlson, K. D.; Ferraro, J. R.; Williams, J. M.; Cariss, C. S.; Rubinstein, R. L.; Withworth, J. R. *Chem. Mater.* **1989**, *1*, 140.
(13) Kobayashi, A.; Kim, H.; Sasaki, Y.; Moriyama, S.; Nishio, Y.; Kayita, K.; Sasaki, W.; Kato, R.; Kobayashi, H. *Chem. Lett.* **1987**, 1819.
(14) Kobayashi, H.; Kato, R.; Kobayashi, A. *Synth. Met.* **1991**, *42*, 2495.
(15) Lakshmikantham, M. V.; Cava, M. P. *J. Org. Chem.* **1980**, *45*, 2632.
(16) Steimecke, G.; Sieler, H. J.; Kirmse, R.; Hoyer, E. *Phosphorus Sulfur* **1979**, *7*, 49.
(17) Klayman, D. L.; Griffin, S. L. *J. Am. Chem. Soc.* **1973**, *95*, 197.

Table I. Crystallographic Data for I and II

compd	I	II
empirical formula	$C_{16}H_{12}NNi_2S_{16}Se_4$	$C_{16}H_{12}NNi_2S_{16}Se_4$
fw	1164.48	1164.48
space group	*Pbnb* (No. 56)	*C*2/*c* (No. 15)
a, Å	7.3617(7)	14.1465(7)
b, Å	11.6824(9)	6.4999(4)
c, Å	39.004(2)	36.553(2)
α, deg	90	90
β, deg	90	95.580(4)
γ, deg	90	90
V, Å^3	3354.4(4)	3345.1(3)
Z	4	4
ρ(calcd), g cm^{-3}	2.306	2.312
μ(Mo Kα), cm^{-1}	64.0	64.2
T, K	300	300
λ(Mo Kα), Å	0.710 73	0.710 73
R^a	0.072	0.057
$R_w{}^b$	0.072	0.051

^{a} $R = \sum(|F_o| - |F_c|)/\sum|F_o|$. ^{b} $R_w = [\sum w(|F_o| - |F_c|)^2/\sum w|F_o|^2]^{1/2}$; $w = 1/\sigma^2(F)$.

platelets of the α-phase. The two phases could be easily separated manually. The stoichiometry of both phases was deduced from the X-ray analyses.

X-ray Structure Determination of I and II. X-ray data were collected at room temperature on an Enraf-Nonius CAD-4T/rotating anode (50 kV, 200 mA) diffractometer for a black, platelet-shaped crystal of dimensions 0.02 × 0.3 × 0.3 mm^3 (I) or a black, rod-shaped crystal of dimensions 0.53 × 0.06 × 0.013 mm^3 (II) mounted inside Lindemann glass capillaries. Graphite-monochromated Mo Kα (λ = 0.710 73 Å) radiation was used. Crystal data and numerical details on the structure determinations have been collected in Table I. Unit cell parameters were calculated from the SET4 setting angles for 25 reflections ($9 < \theta < 12°$ for I; $6.5 < \theta < 17°$ for II). The small crystals reflected relatively poorly, even at 10 kW, in particular at higher θ angles. However, the ratios of the number of observed reflections to the number of parameters (≈ 10) were considered acceptable for these analyses. A total of 6919 reflections (for I) of which 1909 with $I > 3\sigma(I)$ were considered observed, and 4666 reflections (for II) of which 1762 with $I > 2.5\sigma(I)$ were considered observed, were collected by the $\omega/2\theta$ scan technique up to $\theta = 27.5°$ (for I and II). They were corrected for Lorentz and polarization effects. Absorption correction was applied using empirical methods[18] (DIFABS correction range 0.49–1.29 for I; 0.41–1.30 for II). The intensity data were merged into unique data sets (R_{int} = 0.06 for I, 0.055 for II). Both structures were solved by direct methods (SHELXS-86/TREF).[19] Refinement on *F* was carried out by full-matrix least-squares methods (SHELX-76).[20] All non-hydrogen atoms were refined anisotropically. The hydrogen atoms were accounted for at calculated positions with *d*(C–H) = 0.98 Å. Weights based on counting statistics were introduced in the final refinement cycles. The final *R* values were 0.072 (for I) and 0.057 (for II), while the values for R_w were 0.072 (for I) and 0.051 (for II). Atomic fractional coordinates and equivalent thermal parameters for the non-hydrogen atoms of I and II are presented in Tables II and III, respectively. Scattering factors were taken from ref 21, and were corrected for anomalous dispersion.[22] Geometrical calculations were done with the program PLATON.[23] All calculations were carried out on a DEC5000 system.

Cyclic Voltammetry Studies. All electrochemical measurements were performed by using a DACFAMOV 05-03 instrument.[24,25] The electrochemical cell used for cyclic voltammetry employed a platinum working electrode, a platinum wire as the auxiliary electrode, and a Ag/AgCl (in 0.1 N KCl) reference electrode. Measurements were carried out on acetonitrile solutions containing 10^{-3} M $[Bu_4N]_2[M(dmise)_2]$, (M = Ni, Pd) with use of 0.1 M Bu_4NPF_6 as supporting electrolyte. Argon was passed through the solution prior to taking the measurements and an argon blanket was maintained above the solution during experiments.

Table II. Final Coordinates and Equivalent Isotropic Thermal Parameters of the Non-Hydrogen Atoms for α-$[Me_4N][Ni(dmise)_2]_2$ (I)

atom	*x*	*y*	*z*	*U*(eq),^{a} Å^2
Ni	0.6624(3)	0.5884(2)	0.02965(5)	0.0220(5)
Se(1)	0.7350(4)	0.4231(2)	0.20809(5)	0.0694(9)
Se(2)	0.6544(3)	0.7416(2)	–0.14959(5)	0.0690(9)
S(1)	0.7925(6)	0.4489(3)	0.05629(9)	0.030(1)
S(2)	0.8197(7)	0.3925(4)	0.1316(1)	0.036(2)
S(3)	0.6106(7)	0.5878(4)	0.1508(1)	0.041(2)
S(4)	0.5647(6)	0.6648(3)	0.0768(1)	0.029(1)
S(5)	0.5471(6)	0.7296(3)	0.0013(1)	0.028(1)
S(6)	0.5568(6)	0.7871(4)	–0.0742(1)	0.035(1)
S(7)	0.7516(7)	0.5794(4)	–0.09011(9)	0.032(1)
S(8)	0.7599(7)	0.5065(3)	–0.01633(9)	0.028(1)
C(1)	0.746(2)	0.477(1)	0.0986(3)	0.025(4)
C(2)	0.724(2)	0.467(1)	0.1627(3)	0.026(5)
C(3)	0.647(2)	0.571(1)	0.1069(3)	0.019(4)
C(4)	0.610(2)	0.700(1)	–0.0401(3)	0.019(4)
C(5)	0.658(2)	0.706(1)	–0.1044(4)	0.035(5)
C(6)	0.702(2)	0.600(1)	–0.0467(3)	0.019(4)
N	1/4	0.107(2)	1/4	0.055(9)
C(7)	0.228(4)	0.035(2)	0.2806(4)	0.070(9)
C(8)	0.092(3)	0.184(2)	0.2448(8)	0.09(1)

^{a} *U*(eq) = one-third of the trace of the orthogonalized U.

Table III. Final Coordinates and Equivalent Isotropic Thermal Parameters of the Non-Hydrogen Atoms for β-$[Me_4N][Ni(dmise)_2]_2$ (II)

atom	*x*	*y*	*z*	*U*(eq),^{a} Å^2
Ni	0.3651(1)	0.1268(2)	0.01894(4)	0.0288(5)
Se(1)	0.2816(1)	0.3549(3)	0.20680(4)	0.0614(7)
Se(2)	0.4322(1)	–0.1661(3)	–0.16729(4)	0.0649(7)
S(1)	0.3258(2)	–0.0567(5)	0.06442(9)	0.037(1)
S(2)	0.2943(2)	0.0581(5)	0.14211(9)	0.037(1)
S(3)	0.3340(2)	0.4856(5)	0.12998(9)	0.038(1)
S(4)	0.3706(2)	0.4089(5)	0.05033(8)	0.036(1)
S(5)	0.3618(2)	–0.1602(5)	–0.01047(8)	0.037(1)
S(6)	0.3922(2)	–0.2607(5)	–0.08864(8)	0.039(1)
S(7)	0.4304(2)	0.1623(6)	–0.10567(8)	0.040(1)
S(8)	0.4034(2)	0.3005(5)	–0.02824(9)	0.040(1)
C(1)	0.3212(7)	0.121(2)	0.0984(3)	0.029(4)
C(2)	0.3043(8)	0.302(2)	0.1596(3)	0.037(5)
C(3)	0.3415(7)	0.327(2)	0.0922(3)	0.031(4)
C(4)	0.3873(7)	–0.088(2)	–0.0524(3)	0.028(4)
C(5)	0.4185(8)	–0.087(2)	–0.1204(3)	0.038(5)
C(6)	0.4045(8)	0.115(2)	–0.0614(3)	0.030(4)
N	0	0.247(2)	1/4	0.036(5)
C(7)	–0.0298(8)	0.122(2)	0.2798(3)	0.049(5)
C(8)	0.0812(8)	0.384(2)	0.2643(3)	0.048(5)

^{a} *U*(eq) = one-third of the trace of the orthogonalized U.

Results and Discussion

Description of the X-ray Structure of I. Table IV lists all relevant bond distances and bond angles for compound I. The crystallographically independent molecule consists of one Ni(dmise)$_2$ unit and half of the Me_4N^+ cation, with the nitrogen atom lying on a 2-fold axis. The labeling scheme used is shown in Figure 1; this scheme is also valid for compound II (vide infra).

In Figure 2 the unit cell contents of the structure of I are depicted. The α-phase of $[Me_4N][Ni(dmise)_2]_2$ is isostructural with $[Me_4P][Ni(dmit)_2]_2$ and $[Me_4As][Ni(dmit)_2]_2$.[26] In compound I, the Ni(dmise)$_2$ anions do not form stacks, as is normally the case in M(dmit)$_2$ salts,[2] but are arranged in dimers ("diads") which make an angle of 63° with four of their six neighboring dimers (see Figure 4). The intradimer spacing is 3.50 Å. This spacing is larger than the one found in $[Me_4P][Ni(dmit)_2]_2$ and $[Me_4As][Ni(dmit)_2]_2$, i.e. 3.32–3.33 Å,[26] indicating that in

(18) Walker, N.; Stuart, D. *Acta Crystallogr.* **1983**, *A39*, 158.
(19) Sheldrick, G. M. SHELXS-86, Program for Crystal Structure Determinations. University of Göttingen, FRG, 1986.
(20) Sheldrick, G. M. SHELX-76, Program for Crystal Structure Determinations. University of Cambridge, U.K., 1976.
(21) Cromer, D. T.; Mann, J. B. *Acta Crystallogr., Sect. A* **1968**, *24*, 321.
(22) Cromer, D. T.; Liberman, D. *J. Phys. Chem.* **1970**, *53*, 1891.
(23) Spek, A. L. *Acta Crystallogr., Sect. A* **1990**, *46*, C34.
(24) Cassoux, P.; Dartiguepeyron, R.; Fabre, P.-L.; de Montauzon, D. *Actual. Chim.* **1985**, 79.
(25) Cassoux, P.; Dartiguepeyron, R.; Fabre, P.-L.; de Montauzon, D. *Electrochim. Acta* **1985**, *11*, 1485.
(26) Kato, R.; Kobayashi, H.; Kim, H.; Kobayashi, A.; Sasaki, Y.; Mori, T.; Inokuchi, H. *Synth. Met.* **1988**, *27*, B359.

Table IV. Bond Distances (Å) and Angles (deg) for α-$[Me_4N][Ni(dmise)_2]_2$ (I)

Ni–S(1)	2.157(4)	S(4)–C(3)	1.71(1)
Ni–S(4)	2.168(5)	S(5)–C(4)	1.71(1)
Ni–S(5)	2.160(4)	S(6)–C(4)	1.72(1)
Ni–S(8)	2.156(4)	S(7)–C(6)	1.75(2)
Se(1)–C(2)	1.85(1)	S(8)–C(6)	1.66(1)
Se(2)–C(5)	1.81(2)	C(1)–C(3)	1.36(2)
S(1)–C(1)	1.72(1)	C(4)–C(6)	1.38(2)
S(2)–C(1)	1.71(1)	S(6)–C(5)	1.69(2)
S(2)–C(2)	1.65(1)	S(7)–C(5)	1.72(2)
S(3)–C(2)	1.70(2)	N–C(7)	1.47(2)
S(3)–C(3)	1.74(1)	N–C(8)	1.48(3)
S(1)–Ni–S(4)	92.8(2)	S(6)–C(4)–C(6)	118.1(9)
S(1)–Ni–S(5)	176.6(2)	Se(2)–C(5)–S(6)	122.8(9)
S(1)–Ni–S(8)	85.3(2)	Se(2)–C(5)–S(7)	121.3(9)
S(4)–Ni–S(5)	89.4(2)	S(6)–C(5)–S(7)	115.7(9)
S(4)–Ni–S(8)	117.9(2)	S(7)–C(6)–S(8)	123.3(9)
S(5)–Ni–S(8)	92.5(2)	S(7)–C(6)–C(4)	113(1)
Ni–S(1)–C(1)	103.2(5)	S(8)–C(6)–C(4)	123.3(9)
C(1)–S(2)–C(2)	96.4(7)	C(7)–N–C(8)	112(2)
C(2)–S(3)–C(3)	95.8(7)	C(7)–N–C(7a)	110(2)
Ni–S(4)–C(3)	101.6(5)	C(7)–N–C(8a)	109(2)
Ni–S(5)–C(4)	102.8(5)	C(7a)–N–C(8)	109(2)
C(4)–S(6)–C(5)	96.1(7)	C(8)–N–C(8a)	106(2)
C(5)–S(7)–C(6)	96.6(7)	C(7a)–N–C(8a)	112(2)
Ni–S(8)–C(6)	102.6(5)	S(5)–C(4)–C(6)	119(1)
S(2)–C(2)–S(3)	116.5(7)	S(1)–C(1)–S(2)	123.0(9)
S(3)–C(3)–S(4)	123.2(8)	S(1)–C(1)–C(3)	120(1)
S(3)–C(3)–C(1)	114(1)	S(2)–C(1)–C(3)	117.4(9)
S(4)–C(3)–C(1)	122.8(9)	Se(1)–C(2)–S(2)	122.7(9)
S(5)–C(4)–S(6)	123.1(9)	Se(1)–C(2)–S(3)	120.9(8)

Table V. Bond Distances (Å) and Angles (deg) for β-$[Me_4N][Ni(dmise)_2]_2$ (II)

Ni–S(1)	2.162(4)	S(4)–C(3)	1.71(1)
Ni–S(4)	2.160(3)	S(5)–C(4)	1.68(1)
Ni–S(5)	2.151(3)	S(6)–C(4)	1.74(1)
Ni–S(8)	2.174(4)	S(6)–C(5)	1.69(1)
Se(1)–C(2)	1.82(1)	S(7)–C(5)	1.71(1)
Se(2)–C(5)	1.82(1)	S(7)–C(6)	1.72(1)
S(1)–C(1)	1.70(1)	S(8)–C(6)	1.71(1)
S(2)–C(1)	1.73(1)	C(1)–C(3)	1.40(2)
S(2)–C(2)	1.71(1)	C(4)–C(6)	1.39(2)
S(3)–C(2)	1.69(1)	N–C(7)	1.45(1)
S(3)–C(3)	1.73(1)	N–C(8)	1.51(1)
S(1)–Ni–S(4)	93.4(1)	S(6)–C(4)–C(6)	114.3(8)
S(1)–Ni–S(5)	84.9(1)	Se(2)–C(5)–S(6)	120.6(7)
S(1)–Ni–S(8)	177.7(1)	Se(2)–C(5)–S(7)	123.3(7)
S(4)–Ni–S(5)	177.8(1)	S(6)–C(5)–S(7)	116.1(6)
S(4)–Ni–S(8)	88.9(1)	S(7)–C(6)–S(8)	124.0(7)
S(5)–Ni–S(8)	92.8(1)	S(7)–C(6)–C(4)	116.7(8)
Ni–S(1)–C(1)	102.6(4)	S(8)–C(6)–C(4)	119.2(8)
C(1)–S(2)–C(2)	96.3(5)	C(7)–N–C(8)	109.7(6)
C(2)–S(3)–C(3)	97.4(6)	C(7)–N–C(7a)	112(1)
Ni–S(4)–C(3)	102.3(4)	C(7)–N–C(8a)	108.9(6)
Ni–S(5)–C(4)	102.6(4)	C(7a)–N–C(8)	108.9(6)
C(4)–S(6)–C(5)	96.9(6)	C(8)–N–C(8a)	108(1)
C(5)–S(7)–C(6)	96.0(6)	C(7a)–N–C(8a)	109.7(6)
Ni–S(8)–C(6)	102.5(4)	S(2)–C(2)–S(3)	115.6(6)
S(1)–C(1)–S(2)	122.9(7)	S(3)–C(3)–S(4)	124.6(7)
S(1)–C(1)–C(3)	120.7(8)	S(3)–C(3)–C(1)	114.3(8)
S(2)–C(1)–C(3)	116.4(8)	S(4)–C(3)–C(1)	121.0(9)
Se(1)–C(2)–S(2)	120.9(7)	S(5)–C(4)–S(6)	123.0(7)
Se(1)–C(2)–S(3)	123.5(7)	S(5)–C(4)–C(6)	122.7(9)

compound I the anions are less strongly dimerized. The intradimer Ni···S(8) distance is relatively short, namely 3.341 (5) Å. Figure 6 shows the mode of intermolecular overlap within a dimer. Short S···S contacts exist predominantly between the $[Ni(dmise)_2]_2$ dimers. They build a two-dimensional network in the *ab* plane. Table VI lists all intermolecular contacts shorter than the sum of the van der Waals radii in structure I.

This nonstacking arrangement of loosely dimerized molecules can be compared to the κ-phase $(BEDT\text{-}TTF)_2X$ salts (BEDT-TTF = bis(ethylenedithio)tetrathiafulvalene and X = linear inorganic anion), where the organic units also form layers consisting of $(BEDT\text{-}TTF)_2$ dimers which are oriented nearly orthogonal to one another. Many κ-phase $(BEDT\text{-}TTF)_2X$ salts exhibit superconductivity at ambient pressure.[27]

As expected from the larger size of the selenium atoms, the unit-volume of α-$[Me_4N][Ni(dmise)_2]_2$ is somewhat larger (on

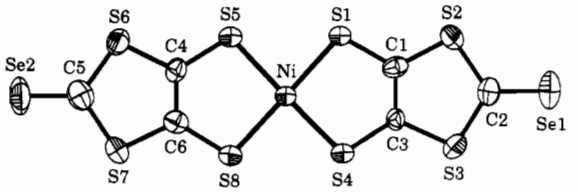

Figure 1. ORTEP plot of the $Ni(dmise)_2$ unit (50% probability level).

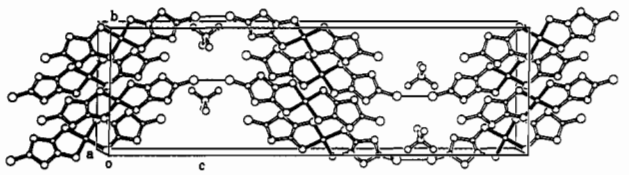

Figure 2. Unit-cell contents of structure I. Single black lines represent short Se···Se contacts.

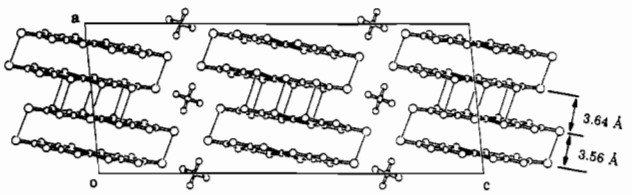

Figure 3. Unit-cell contents of structure II. Single black lines represent short chalcogen···chalcogen contacts.

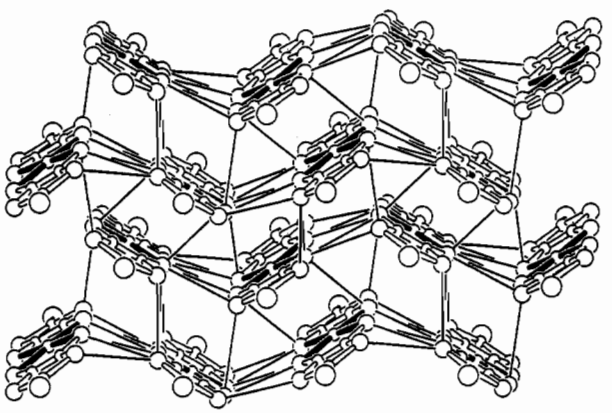

Figure 4. Layer of $Ni(dmise)_2$ molecules in I. Single black lines represent short S···S contacts.

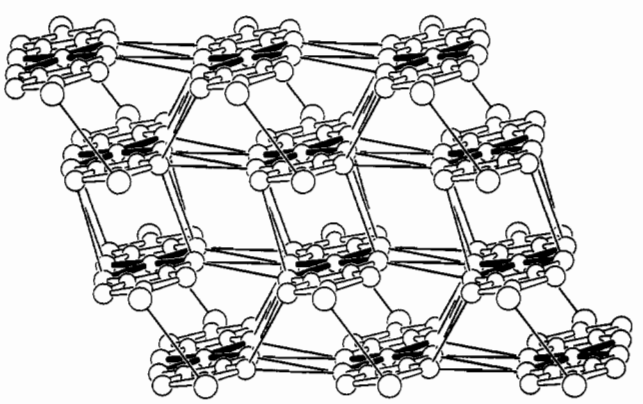

Figure 5. Layer of $Ni(dmise)_2$ molecules in II. Single black lines represent short chalcogen···chalcogen contacts.

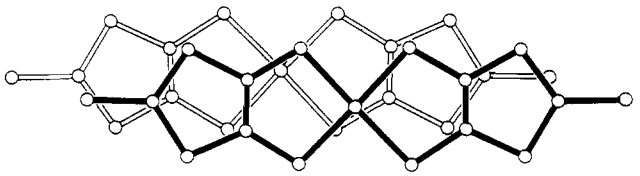

Figure 6. Intradimer overlapping of $Ni(dmise)_2$ molecules in **I**.

Table VI. Significant Intermolecular Chalcogen···Chalcogen Contacts in Compound **I**[a]

contact	sym operation	distance, Å
Se(1)···Se(1)	$(-x+1^1/_2, y, -z+{}^1/_2)$	3.277(3)
S(1)···S(4)	$(-x+1^1/_2, y-{}^1/_2, z)$	3.573(5)
S(1)···S(5)	$(-x+1^1/_2, y-{}^1/_2, z)$	3.544(5)
S(1)···S(7)	$(-x+2, -y+1, -z)$	3.621(7)
S(1)···S(8)	$(-x+2, -y+1, -z)$	3.682(6)
S(2)···S(3)	$(-x+1^1/_2, y-{}^1/_2, z)$	3.674(7)
S(2)···S(4)	$(-x+1^1/_2, y-{}^1/_2, z)$	3.515(6)
S(2)···S(7)	$(-x+2, -y+1, -z)$	3.561(7)
S(4)···S(6)	$(x+{}^1/_2, -y+1^1/_2, -z)$	3.668(6)
S(5)···S(8)	$(-x+1^1/_2, y+{}^1/_2, z)$	3.599(5)
S(5)···S(8)	$(-x+1, -y+1, -z)$	3.614(6)
S(6)···S(8)	$(-x+1^1/_2, y+{}^1/_2, z)$	3.671(6)

[a] Symmetry operation applied on second atom.

average 60 Å^3, ≈ 2%) than the unit cell volumes of $[Me_4P][Ni(dmit)_2]_2$ and $[Me_4As][Ni(dmit)_2]_2$[26], even though the Me_4N^+ cation is smaller than Me_4P^+ and Me_4As^+.

A unique feature in the structure of α-$[Me_4N][Ni(dmise)_2]_2$ is the extremely short terminal Se···Se contact of 3.277 (3) Å which connects the acceptor layers along the *c*-axis (Figure 2). This intermolecular contact is more than 0.72 Å shorter than the sum of the van der Waals radii (i.e. 4 Å).

Description of the X-ray Structure of II. Table V lists all relevant bond distances and bond angles for compound **II**. The crystallographically independent unit consists of one nearly planar $Ni(dmise)_2$ molecule and half of the cation. The Me_4N^+ cation is positioned on the 2-fold axis and is therefore in an ordered state. The numbering scheme is given in Figure 1.

The molecular lattice of β-$[Me_4N][Ni(dmise)_2]_2$ is isostructural with that of the all-sulfur analog $[Me_4N][Ni(dmit)_2]_2$.[2,13] The $Ni(dmise)_2$ units are dimerized and form stacks along [110] and [1$\bar{1}$0] (Figure 3). In compound **II**, the two independent interplanar spacings of 3.64 Å and 3.56 Å are larger and differ more from each other than those observed in $[Me_4N][Ni(dmit)_2]_2$ (3.58 Å and 3.53 Å, respectively). Along the stacking directions, short S···S and Se···Se contacts can be found. In Figure 7 the two modes of intermolecular overlap in the stacks are shown. They are identical to the intermolecular overlaps found in $[Me_4N][Ni(dmit)_2]_2$.[2,13]

The $Ni(dmise)_2$ columns build layers in the (001) plane which are separated from each other by a sheet of cations. Most short S···S contacts are found to exist between adjacent stacks of $Ni(dmise)_2$ anions (Figure 5). Table VII lists all intermolecular interactions shorter than the sum of the van der Waals radii in structure **II**. The unit-cell volume of β-$[Me_4N][Ni(dmise)_2]_2$ is 106 Å^3 larger (≈ 3%) than that of the corresponding dmit salt.[28]

Conductivity Measurements. The electrical conductivity at ambient pressure was measured on single crystals in the temperature range 300–110 K. The four-probe contact method was used. Gold wires were glued to the crystal surface by gold paint.

For compound **I**, five different crystals were measured. Room-temperature conductivities lie around 1 S cm^{-1}, comparable to the values found for $[Me_4P][Ni(dmit)_2]_2$ and $[Me_4As][Ni(dmit)_2]_2$. Upon lowering temperature, the conductivity of most samples decreases slowly until approximately 140 K. For one crystal, however, a weakly metallic behavior down to 140 K was observed.[5d] After this point the conductivity falls rapidly in all cases. The value for the activation energy proved to be 0.08 eV. A similar semiconducting behavior was found for $[Me_4P][Ni(dmit)_2]_2$ and $[Me_4As][Ni(dmit)_2]_2$. Low-temperature (77 K) single-crystal X-ray measurements were carried out to check if a phase transition or a lattice incommensurability occurs around 140 K. However, no signs of a structural modulation could be found.

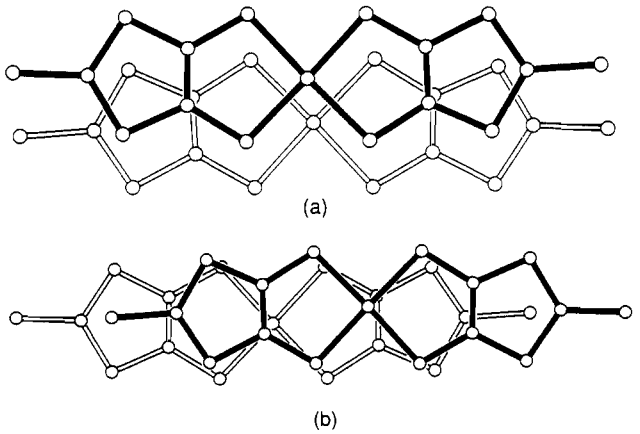

Figure 7. Modes of intermolecular overlapping of $Ni(dmise)_2$ molecules in **II**: (a) intradimer; (b) interdimer.

Table VII. Significant Intermolecular Chalcogen···Chalcogen Contacts in Compound **II**[a]

contact	sym operation	distance, Å
Se(1)···Se(2)	$(-x+{}^1/_2, -y+{}^1/_2, -z)$	3.805(2)
S(1)···S(4)	$(x, y-1, z)$	3.577(5)
S(1)···S(7)	$(-x+1, -y, -z)$	3.692(4)
S(1)···S(5)	$(-x+{}^1/_2, -y-{}^1/_2, -z)$	3.647(4)
S(1)···S(6)	$(-x+{}^1/_2, -y-{}^1/_2, -z)$	3.498(4)
S(2)···S(6)	$(-x+{}^1/_2, -y-{}^1/_2, -z)$	3.676(4)
S(4)···S(5)	$(x, y+1, z)$	3.570(4)
S(4)···S(6)	$(-x+1, -y, -z)$	3.638(4)
S(5)···S(8)	$(x, y-1, z)$	3.624(5)
S(5)···S(8)	$(-x+1, -y, -z)$	3.599(4)
S(5)···S(5)	$(-x+{}^1/_2, -y-{}^1/_2, -z)$	3.525(4)
S(6)···S(8)	$(x, y-1, z)$	3.601(5)

[a] Symmetry operation applied on second atom.

For compound **II**, three different crystals were measured, each of which exhibited a semiconducting behavior. The room-temperature conductivity measured along the needle axis (corresponding to the *b*-axis in the unit cell) has a value of approximately 10 S cm^{-1}, which is roughly 5 times lower than the room-temperature conductivity of $[Me_4N][Ni(dmit)_2]_2$.[29] No transition point was observed. Activation energies were found to be small, around 0.05 eV.[30] The fact that β-$[Me_4N][Ni(dmise)_2]_2$ is apparently a semiconductor at ambient pressure is in sharp contrast with the metallic behavior of its all-sulfur analog $[Me_4N][Ni(dmit)_2]_2$.[11,29]

Intermolecular Overlap Integral Calculations. The intermolecular orbital overlaps (S) between the LUMO's (lowest unoccupied molecular orbital) of neighboring $Ni(dmise)_2$ units were calculated using the scheme described in ref 31. The molecular orbitals of the neutral $Ni(dmise)_2$ were calculated using

(27) Williams, J. M.; Schultz, A. J.; Geiser, U.; Carlson, K. D.; Kini, A. M.; Wang, H. H.; Kwok, W.-K.; Whangbo, M.-H.; Schirber, J. E. *Science* **1991**, *252*, 1501 and references therein.
(28) Kobayashi, A.; Kim, H.; Sasaki, Y.; Moriyama, S.; Nishio, Y.; Kajita, K.; Sasaki, W.; Kato, R.; Kobayashi, H. *Chem. Lett.* **1987**, 1799.
(29) Kobayashi, A.; Kim, H.; Sasaki, Y.; Kato, R.; Kobayashi, H.; Moriyama, S.; Nishio, Y.; Kajita, K.; Sasaki, W. *Chem. Lett.* **1987**, 1819.
(30) Cornelissen, J. P. Ph.D. Thesis, Leiden University, The Netherlands, 1992.
(31) (a) Kramer, G. J. Ph.D. Thesis, Leiden University, The Netherlands, 1988. (b) Roothaan, C. C. J. *J. Chem. Phys.* **1951**, *19*, 1445.

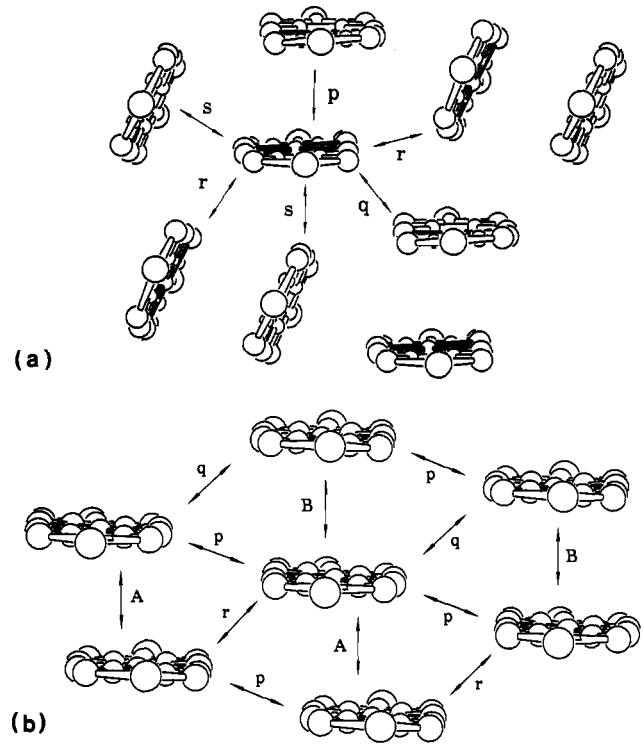

Figure 8. (a) Scheme of the intermolecular overlap integrals of the LUMO's of the acceptor molecules in compound **I**. Absolute overlap integral values ($\times 10^3$): p, 6.7; q, 6.2; r, 1.6; s, 0.2. (b) Scheme of the intermolecular overlap integrals (S) of the LUMO's of the acceptor molecules in compound **II**. Absolute overlap integral values ($\times 10^3$): A, 18; B, 1.1; p, 0.2; q, <0.1; r, 6.

the extended Hückel program ICON8,[32] with semiempirical parameters taken from refs 33 and 34. In Figure 8 the letters A, B, p, q, r, s represent the intermolecular orbital overlaps for compounds **I** and **II**, respectively. The values of these integrals are given in the caption of Figure 8.

Not surprisingly, the electronic systems of the two structures differ substantially. In the lattice of α-$[Me_4N][Ni(dmise)_2]_2$ the largest overlap occurs between the two anions of one dimer (p), as was the case for $[Me_4P][Ni(dmit)_2]_2$ and $[Me_4As][Ni(dmit)_2]_2$.[26] The overlap integral between two neighboring dimers in the *ab* plane lying parallel to each other (q) is almost as large. The value of the overlap integrals in the *ab* plane between pairs making an angle of 63° with one another (r) is also significant, approximately one-fourth of the value for q. The electronic system of **I** bears close resemblance to the one found for the isostructural $[Me_4P][Ni(dmit)_2]_2$ and $[Me_4As][Ni(dmit)_2]_2$ salts.[26] Although the distance between the selenonyl groups along the *c*-axis is very short, the large overlap angle of 63° results in a low value for the transfer integral. In conclusion, compound **I** is rather well described as a (quasi-) 1-D conductor. This is in contrast to the 2-D character of the conduction pathway in the κ-phase BEDT-TTF salts.[27]

The electronic system of β-$[Me_4N][Ni(dmise)_2]_2$ is more or less "conventional". The orbital overlap (A) between the $Ni(dmise)_2$ units which make up the dimers is the largest occurring in the lattice. Its value is almost 20 times larger than the interdimer overlap in the stacking direction (B), even though a larger number of intermolecular contacts appears to be present between each two dimers. Comparing these data with the integral values calculated for $[Me_4N][Ni(dmit)_2]_2$, where A and B are of equal size,[28] it is obvious that from an electronic point of view the $Ni(dmise)_2$ stacks should be considered more dimerized than the $Ni(dmit)_2$ stacks in $[Me_4N][Ni(dmit)_2]_2$. This was not unexpected, given the larger difference in interplanar spacings (see Figure 3). Significant side-by-side overlaps are present, too, of which the most important (r) is about one-third of the intradimer overlap (A). The overlap between the seleno groups along the *c*-axis is virtually negligible.

Table VIII. Electrochemical Potentials (V) vs Ag/AgCl in 0.1 N KCl for $[M(C_3S_ySe_{5-y})_2]$ Systems (M = Ni, Pd; $y \leq 5$)

compd	$E_{1/2}$ ($M^{II} \rightleftharpoons M^{III}$)	E_{ox} ($M^{III} \rightarrow M^{IV}$)	E_{red} ($M^{IV} \rightarrow M^{III}$)	ref
$[Bu_4N]_2[Ni(dmit)_2]$[a]	-0.15	0.21	0.10	35a
$[Bu_4N]_2[Ni(dmise)_2]$[a]	-0.13	0.21	0.12	
$[Bu_4N]_2[Ni(dsit)_2]$[b]	-0.12	0.183	0.08, -0.01	10
$[Bu_4N]_2[Ni(dsise)_2]$[c]	-0.166	not reported	not reported	9
$[Bu_4N]_2[Pd(dmit)_2]$[a]	0.05	0.2		35b
$[Bu_4N]_2[Pd(dmise)_2]$[a]		0.001	-0.057	
$[Bu_4N]_2[Pd(dsit)_2]$[a]		0.01	-0.092	30
$[Bu_4N]_2[Pd(dsise)_2]$[c]		not reported	not reported	9

[a] In CH_3CN. [b] In acetone. [c] In DMF/CH_3CN (3:2).

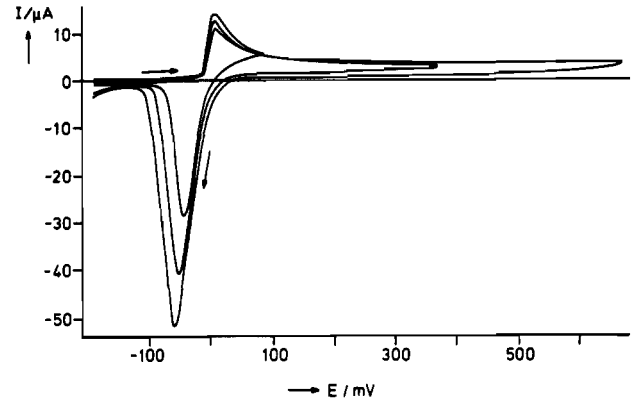

Figure 9. Cyclic voltammogram of $[Bu_4N]_2[Pd(dmise)_2]$ (10^{-3} M in CH_3CN, Bu_4NPF_6, 0.1 V/s).

Cyclic Voltammetry. Solutions of $[Bu_4N]_2[Ni(dmise)_2]$ in acetonitrile show a reversible first wave, corresponding to the $[Ni(dmise)_2]^{2-}/[Ni(dmise)_2]^-$ couple, at $E_{1/2} = -0.13$ V vs Ag/AgCl in 0.1 N KCl (Table VIII). A second peak which consists of an abrupt increase of the current intensity (anodic peak at +0.21 V vs Ag/AgCl in 0.1 N KCl) may be attributed to the irreversible $[Ni(dmise)_2]^-/[Ni(dmise)_2]^{x-}$ couple. Furthermore, the intensity of the corresponding cathodic peak, which is found at +0.12 V, strongly increases after more than one cycle. These phenomena are usually explained by assuming the deposition of a conducting species on the electrode during the oxidation process.[35] The shapes of the redox couples are identical to those found for the $[Bu_4N]_2[Ni(dmit)_2]$ system, as described in the literature.[35a] The potential of the reversible $[Ni(dmise)_2]^{2-}/[Ni(dmise)_2]^-$ wave is slightly higher than the $E_{1/2}$ value found for the corresponding dmit salt (-0.15 V), but lower than that for the $Ni(dsit)_2$ system ($E_{1/2} = -0.12$ V in acetone).[10] These data are in agreement with the observation reported by Olk et al.[9] that the oxidation from Ni^{II} to Ni^{III} becomes more difficult as the number of Se atoms in the ligand increases.

The cyclic voltammogram of $[Bu_4N]_2[Pd(dmise)_2]$ is depicted in Figure 9. When scanning back and forth between -0.4 and +0.7 V, only *one* (irreversible) couple can be found. Its anodic peak has a maximum at 0 V, and the corresponding reduction step occurs at -0.06 V (Table VIII). The shape of the couple, as well as the increasing intensity of the cathodic peak after

(32) Howell, J.; Rossi, A.; Wallace, D.; Haraki, K.; Hoffmann, R. ICON8 and FORTICON8, QCPE, Program for Extended Hückel Calculations.
(33) McGlynn, S. P., Vanquickenborne, L. G., Konoshita, M., Carroll, D. G., Eds. *Introduction to Applied Quantum Chemistry*; Holt, Rhinehart and Winston Inc.: New York, 1972.
(34) Ballhausen, C. J., Gray, H. B., Eds.; *Molecular Orbital Theory*; W. A. Benjamin, Inc.: New York, 1964.
(35) (a) Valade, L.; Cassoux, P.; Gleizes, A.; Interrante, L. V. *J. Phys. Colloq.* **1983**, *44C3*, 1183. (b) Valade, L. Ph.D. Thesis, Toulouse, France, 1987. (c) Valade, L.; Bousseau, M.; Cassoux, P. *Nouv. J. Chim.* **1985**, *9*, 351.

numerous cycles, is very similar to that of the $[Ni(dmise)_2]^{-}/[Ni(dmise)_2]^{x-}$ couple. Compared to the electrochemical behavior of $[Bu_4N]_2[Pd(dmit)_2]$[35a], the cyclic voltammogram of $[Bu_4N]_2[Pd(dmise)_2]$ is radically different. Electrochemical studies on acetonitrile solutions of $[Bu_4N]_2[Pd(dmit)_2]$ showed a two-stage oxidation process consisting of a clear, reversible $[Pd(dmit)_2]^{2-}/[Pd(dmit)_2]^{-}$ wave at $E_{1/2} = +0.05$ V (vs Ag/AgCl in 0.1 N KCl) and a second oxidation step at +0.20 V, rather similar to the cyclic voltammogram of $[Bu_4N]_2[Ni(dmit)_2]$. For $[Bu_4N]_2[Pd(dmise)_2]$ the entire oxidation process from $[Pd(dmise)_2]^{2-}$ to $[Pd(dmise)_2]^{x-}$ seems to occur in only one step at a relatively low potential. The absence of a reversible Pd^{II}/Pd^{III} couple has also been observed in the cyclic voltammograms of the $Pd(dsit)_2$[10] and $Pd(dsise)_2$ (dsise = $C_3S_2Se_3^{2-}$ = 1,3-dithiole-2-selenone-4,5-diselenolate) systems (Table VIII).[9]

Concluding Remarks. Single-crystal X-ray determinations have revealed that at least two modifications of $[Me_4N][Ni(dmise)_2]_2$ exist. The α-phase proves to be isostructural with $[Me_4P][Ni(dmit)_2]_2$ and $[Me_4As][Ni(dmit)_2]_2$, while the β-phase is isostructural with $[Me_4N][Ni(dmit)_2]_2$. This indicates that the bulkier character of the seleno group in dmise does not give rise to very different packing motifs of the acceptor units, in contrast to other Se derivatives like $[Me_4N][Ni(dsit)_2]_2$.[8] Still, the relatively minor structural differences which *do* exist appear to have a large influence on the electronic properties of α- and β-$[Me_4N][Ni(dmise)_2]_2$ compared to their dmit analogs. In particular, the spacing between the stacked $Ni(dmise)_2$ units increases when going from a C=S to a C=Se group. This is reflected both in the values of the transfer integrals and in the conductivity behavior of the dmise compounds.

Cyclic voltammetry measurements show that substitution of the thio function in dmit by a seleno group affects the redox properties of the nickel chelate only marginally. The redox behavior of $[Pd(dmise)_2]^{2-}$, however, differs significantly from that of the $[Pd(dmit)_2]$ system. Similar to the oxidation process observed for $[Pd(dsit)_2]^{2-}$,[10] the oxidation to the mixed-valence state occurs in one step, *without* going through a reversible Pd^{II}/Pd^{III} state. Indeed, this appears to be a common feature for all members of the family $[Pd(C_3S_ySe_{5-y})_2]^{2-}$ (with $y < 5$).[9]

The most striking aspect of the present study appears to be the fact that β-$[Me_4N][Ni(dmise)_2]_2$ behaves only as a semiconductor (albeit with a very small activation energy), whereas the all-sulfur salt $[Me_4N][Ni(dmit)_2]_2$ is metallic down to 100 K at ambient pressure, and one sample even becomes superconducting at 5 K under a pressure of 7 kbar.[11] The origin of the relatively poor conductivity of **II** is probably the larger interplanar spacings between the $Ni(dmise)_2$ units, since this is the only feature in compound **II** which differs from that of $[Me_4N][Ni(dmit)_2]_2$. Obviously, a larger distance between the anions results in smaller S···S orbital overlaps, something which is not compensated for by the occurrence of significant Se···Se contacts.

It should be recalled, however, that the conductivity measurements on the crystals of compounds **I** and **II** so far have only been performed at atmospheric pressure. Applying higher pressures is known to increase orbital overlaps and can transform a compound which shows only semiconducting behavior at ambient pressure into a metallic conductor and even a superconductor.[3]

Acknowledgment. The authors are indebted to Dr. C. Faulmann (LCC-CNRS, Toulouse) for assistence with the conductivity measurements and Mr. D. de Montauzon (LCC-CNRS, Toulouse) for assistance with the cyclic voltammetry experiments. Dr. J. de Boer (Groningen University) carried out the low-temperature X-ray measurements. J.P.C. wishes to thank Ms. R.-M. Olk (Karl Marx University, Leipzig, Germany) for helpful discussions. We are grateful to NWO/SON (Nederlandse organisatie voor Wetenschappelijk Onderzoek) and to the CNRS (Centre National de la Recherche Scientifique) in Paris for financial support. This research was in part sponsored by the Werkgroep Fundamenteel Materialen Onderzoek (WFMO).

Supplementary Material Available: Tables of crystal data and details of the structure determinations, atomic coordinates for the hydrogen atoms, thermal parameters of all non-hydrogen atoms and a list of all bond distances and angles for **I** and **II** (10 pages). Ordering information is given on any current masthead page.